International Journal of Applied Pharmaceutics

ISSN- 0975-7058 Vol 18, Issue 2, 2026

Original Article

GREEN-SYNTHESIS OF SILVER NANOPARTICLES USING *N. GLAUCA* LEAVES EXTRACT: CHARACTERIZATION AND EVALUATION OF ANTIOXIDANT, ANTIBACTERIAL AND CYTOTOXIC ACTIVITIES

TABARAK R. AL-SAMMARRAIE[1*], SINA MATALQAH[1], REEM ISSA[2]

[1]Pharmacological and Diagnostic Research Center, Faculty of Pharmacy, Al-Ahliyya Amman University, Amman-19328, Jordan. [2]Faculty of Pharmacy, Middle East University, Amman, Jordan

[*]Corresponding author: Tabarak R. Al-sammarraie; [*]Email: tabarak.r98@gmail.com

Received: 19 Aug 2025, Revised and Accepted: 05 Jan 2026

ABSTRACT

Objective: In this study, silver nanoparticles (NG-AgNPs) were synthesized and characterized using *Nicotiana glauca* (*N. glauca)* leaves extract and their antibacterial and anticancer properties were evaluated.

Methods: An Extract of *N. glauca* leaves was obtained via soxhlet and maceration techniques using water and ethanol as solvents, and the total phenolic content (TPC) and total flavonoid content (TFC) were determined. Water-maceration extract was used to synthesizeNG-AgNPs which were characterized using Ultraviolet-Visible (UV-Vis) spectroscopy, particle size, zeta potential, polydispersity index (PDI), and stability. Antibacterial activity was tested against *Staphylococcus aureus* and *Pseudomonas aeruginosa*, and cytotoxicity was assessed in colorectal (HT-29), lung (A549), and breast (MCF-7) cancer cell lines using an MTT assay.

Results: NG-AgNPs displayed a UV-Vis peak at 440.50 nm, with an average size of 188–280 nm, zeta potential of-29.6 mV, and PDI of 0.216, indicating stability. They demonstrated superior antimicrobial activity with inhibition zones of 24.6 mm (*S. aureus*) and 20.6 mm (*P. aeruginosa*) and Minimum Inhibitory Concentration (MIC) values of 0.15 mg/ml and 0.5 mg/ml, respectively. Cytotoxicity studies revealed IC_{50} values of 2.517µg/ml (HT-29), 25.11 µg/ml (A549), and 24.53µg/ml (MCF-7), while showing no toxicity toward normal endothelial cells (EA. hy926), highlighting their selective cytotoxicity against cancer cells.

Conclusion: These results suggest that the prepared NG-AgNPs exhibit potent antibacterial and anticancer properties with enhanced efficacy compared to the crude extract, making them promising candidates for therapeutic applications.

Keywords: Silver nanoparticles (AgNPs), *Nicotiana glauca*, Green synthesis, Bioactive phytochemicals, Cytotoxicity, Antimicrobial

DOI: https://dx.doi.org/10.22159/ijap.2026v18i2.56577 Journal homepage: https://innovareacademics.in/journals/index.php/ijap

INTRODUCTION

Nicotiana glauca (*N. glauca*), known as "tree tobacco," belongs to the family solanaceae and is an extremely invasive plant that originated in South America [1]. The leaves and flowers of *N. Glauca* have been conventionally utilized in medicine, especially for decoction treatment of jaundice [2]. Recent studies have explored the phytoconstituents of *N. glauca*, showing the presence of alkaloids, including nicotine, in addition to other compounds, such as flavonoids and diterpene glycosides, which may be cytotoxic, antibacterial, and anticancer [3, 4]. Anti-tumor effects of various studies have identified promising cembranoid diterpenes derived from *N. glauca* that inhibit the proliferation of liver and breast cancer cells and induce apoptosis [5, 6]. Extracts from *N. glauca* leaves have also been found to exhibit antimicrobial activity against microorganisms such as Escherichia coli and *S. aureus* [7]. The synthesis of nanoparticles via eco-friendly and sustainable routes has gained significant interest owing to the increasing demand for materials with advanced biomedical and industrial applications. Among these, silver nanoparticles represent a class of NPs that has attracted broad interest because of their impressive antimicrobial, antioxidant, and anticancer activities [8]. Traditional methods of nanoparticle synthesis by chemical and physical processes are usually expensive, laborious, and cause environmental hazards owing to the use of toxic chemicals and the resulting harmful byproducts [9]. Because of these issues, there is a dire need for an alternative through which synthesis can be ensured in an eco-friendly manner. Green synthesis is considered the most effective alternative method, utilizing biological resources, such as plant extracts, bacteria, fungi, and algae, for the synthesis of nanoparticles [10]. The antimicrobial properties of AgNPs are well documented, with biosynthesized AgNPs showing significant activity against a wide range of pathogenic microorganisms, including multidrug-resistant strains. Owing to their small size and large surface area, AgNPs can penetrate bacterial cell walls, leading to membrane disruption, reactive oxygen species (ROS) generation, and inhibition of DNA replication, ultimately resulting in bacterial cell death [11]. In addition to their antimicrobial activity, green-synthesized AgNPs have been shown to possess strong antioxidant properties that are essential for combating oxidative stress and preventing cellular damage [12]. Furthermore, AgNPs synthesized using plant extracts have shown promising anticancer effects by inducing apoptosis in cancer cells, offering potential applications in cancer therapy [13]. The use of *N. glauca* extract for the green synthesis of AgNPs represents a novel approach for producing nanoparticles with enhanced biological activities. The bioactive compounds present in the extract, including phenolic compounds and alkaloids [3, 14], play a crucial role in reducing silver ions to form stable nanoparticles while simultaneously imparting antioxidant, antimicrobial, and anticancer properties to the final product.

While extracts of *N. glauca* have been reported to exhibit cytotoxic and antimicrobial properties, their use as a reducing and capping agent for the green synthesis of silver nanoparticles has not been thoroughly investigated. Furthermore, no study to date has provided a comprehensive evaluation of the stability, antioxidant capacity, antibacterial effects, and selective anticancer activity of *N. glauca*-derived AgNPs. Therefore, this study was designed to address this gap by synthesizing AgNPs using *N. glauca* leaf extract and systematically characterizing their physicochemical and biological properties.

MATERIALS AND METHODS

N. glauca leaves used in this study were harvested from a local nursery in Amman, Jordan. Silver nitrate (99.8% purity) was purchased from Dana Chemicals (Canada). Polyvinylpyrrolidone (PVP) was supplied by Joswe Medical (Jordan). 2,2-Diphenyl-1-picrylhydrazyl (DPPH) free radical (95% purity) was purchased from Sisco Research Laboratories Pvt. Ltd. (India). The 3-(4,5-

Dimethylthiazol-2-yl)-2,5-diphenyltetrazolium bromide (MTT) dye was obtained from Promega (USA). Dulbecco's modified Eagle's medium (DMEM) and RPMI 1640 medium were supplied by Euroclone, Italy. Standard antibiotic disks were obtained from BioAnalytics (Turkey). Mueller-Hinton agar and Mueller-Hinton broth were purchased from Oxoid Ltd. (UK). Pseudomonas aeruginosa ATCC 27853 and Staphylococcus aureus ATCC 29213 were obtained from KWIK-STIK, France.

The instruments used in this study included a Soxhlet extractor (SPL Life Sciences, South Korea), rotary evaporator (Heidolph, Germany), probe sonicator (Sonopuls ultrasonic homogenizer model HD 4000, Bandelin, Germany), Zeta Sizer (Malvern, UK), Ultraviolet-Visible (UV-Vis) spectrophotometer (Shimadzu, Japan), analytical balance (Phoenix Instruments, USA), microcentrifuge (C1015, Centurion Scientific, UK), centrifuge (Electra Medical, US), CO_2 incubator (Thermo Fisher Scientific, USA), deep freezer (Lexicon® II Ultra-low Temperature Freezer, Esco, Singapore), ELISA microplate reader (BioTek Synergy HTX, BioTek, USA), freeze dryer (Zirbus, Germany), hemocytometer (Accuris Instruments, USA), and laminar flow hood (Thermo Fisher Scientific, USA).

Plant material preparation and extraction

The botanical identity of *N. glauca* leaves was confirmed by Dr. Reem Issa (Phytochemistry Specialist, Faculty of Pharmacy, Middle East University). A voucher specimen (*N. glauca* 1/1/2022) of the plant material has been deposited at the Botany Center of Al-Ahliyya Amman University for future reference.

N. glauca leaves were collected, air-dried in a shaded area at room temperature until a constant weight was achieved, and then ground into a uniform powder using an electric mill. Two different extraction techniques, Soxhlet extraction and maceration, were employed to extract phytochemicals from *N. glauca* using both water and ethanol as solvents.

Maceration Method: 5 g of dried plant material (5 g) was placed in a glass pot. For water extraction, 500 ml distilled water was added, whereas for ethanol extraction, 500 ml 96% ethanol was used. The mixture was maintained at room temperature for 24 h (ethanol extract) and 48 h (water extract). After extraction, the mixture was cooled for 1 h in a refrigerator, filtered through Whatman No.1 filter paper, and the filtrate was collected.

Soxhlet Extraction: Five grams of dried plant material were placed in a Soxhlet extractor. For water extraction, 500 ml of distilled water was added to the extractor and 500 ml of 96% ethanol was used for ethanol extraction. The extraction process was run for 4 h, allowing the solvent to circulate through the plant material and collect the extracted compounds. The solvent containing the extracted compounds was collected from the Soxhlet reservoir. All the extracts were concentrated under reduced pressure using a rotary evaporator. For the water extracts, the temperature was kept below 60 °C. For ethanol extracts, the temperature was maintained at approximately 40 °C. The concentrated extracts were then weighed, and the extraction yield percentage was calculated as follows:

$$\text{Extraction yield} = \frac{\text{weight of extract}}{\text{weight of dry material}} * 100\% \ldots\ldots (1)$$

The prepared extracts were stored in a refrigerator (4 °C) until further analysis.

Total phenolic content (TPC)

N. glauca extracts were analyzed using the Folin–Ciocalteu colorimetric method, with modifications as per Lawag *et al.* 2023 [15]. A 200 g portion of sodium carbonate was dissolved in 1 L of distilled water to obtain a Na_2CO_3 solution. For the calibration standard, gallic acid was used: 1.1 g of gallic acid was dissolved in 1000 ml of distilled water and sonicated to obtain a stock solution. Serial dilutions were then performed by repeatedly adding 10 ml of the stock solution and 10 ml of distilled water to produce concentrations ranging from 44 µg/ml to 220 µg/ml.

To prepare the sample, a 100 mg aliquot of the dried aqueous and ethanolic extracts was sonicated in 100 ml of deionized water for 10 min. A 5 ml aliquot of the ethanolic solution and 15 ml of the aqueous solution was diluted to a final volume of 100 ml to obtain the working extract solutions (0.05 and 0.015 mg/ml, respectively), concentrations of phenolic content was divided by the working concentrations to normalize the results.

Ten test tubes were used for the assay. Each tube received 15 ml of distilled water and 1 ml of the Folin–Ciocalteu reagent. To each tube, 1 ml of the plant extract solution was added (sample) and a blank tube received 1 ml of distilled water. The remaining eight tubes contained 1 ml of gallic acid standard dilution. After thorough mixing, the tubes were maintained at room temperature for 6 min. Subsequently, 3 ml of the prepared sodium carbonate solution was added to each tube. The mixtures were kept in the dark at 25 °C for 120 min to allow for complete reaction.

The absorbance was recorded at 765 nm using a UV-Vis spectrophotometer. The total phenolic content was determined using a gallic acid standard curve and expressed as milligrams of gallic acid equivalent (GAE) per g of *N. glauca* extract.

Total flavonoid content (TFC)

An aluminum chloride colorimetric method, with slight modifications from Tristantini and Amalia (2019) [16], was used to determine the TFC of *N. glauca*extracts. To prepare the Aluminum Chloride ($AlCl_3$) reagent solution, 10 g of $AlCl_3$ was dissolved in 100 ml of distilled water. A sodium acetate solution (1 M) was prepared by dissolving 8.2034 g of CH_3COONa in 100 ml of distilled water.

Quercetin was used as the standard for flavonoid quantification. A stock solution of 1% (w/v) quercetin was prepared by dissolving 1 g of quercetin in 100 ml of methanol. Eight serial dilutions were prepared by successively mixing 10 ml of quercetin stock solution with 10 ml of methanol to produce concentrations of 10, 5, 2.5, 1.25, 1, 0.625, 0.5, and 0.3125 mg/ml.

For each sample, 125 mg of dried *N. glauca* extract was sonicated for 10 min in 100 ml of deionized water to ensure complete dissolution and to obtain the working extract solutions (1.25 mg/ml), concentrations of flavonoid content was divided by the working concentration.

Ten test tubes were used in the reaction setup: one for the plant extract, eight for the quercetin standard, and one for the blank. Each tube received 1 ml of test solution (extract or quercetin standard). To every tube, 5 ml of distilled water, 3 ml of ethanol, 25 µl** of $AlCl_3$ solution, and 25 µl** of sodium acetate solution were added. The blank tube contained all reagents except extract/quercetin. All tubes were incubated at room temperature in the dark for one hour to allow for color development.

The absorbance was measured at 415 nm using a UV-Vis spectrophotometer. The total flavonoid content was determined using the quercetin calibration curve and reported as milligrams of quercetin equivalent (QE) per g of *N. glauca* extract.

Ultra-high performance liquid chromatography (UHPLC) for analysis of plant constituents

The analysis of plant constituents was performed using UHPLC coupled with mass spectrometry. Stock solution (10 mg/ml) of the plant extract were prepared by dissolving the water maceration extract in Dimethyl Sulfoxide (DMSO) and diluting it with acetonitrile. The samples were dissolved in 2.0 ml) and diluted to 50 ml using acetonitrile. The solutions were centrifuged at 4000 rpm for 2 min, and the supernatant (1.0 ml) was transferred to an autosampler vial. A 3.0 µl** aliquot was injected into the UHPLC system.

Chromatographic separation was conducted using a Bruker Daltonics Elute UHPLC system with a Bruker Solo 2.0 C-18 column (100 mm x 2.1 mm x 2.0 µm). The mobile phase consisted of water with 0.05% formic acid and acetonitrile, at a flow rate of 0.5 ml/min and 40 °C. The gradient program was set as follows: a linear gradient from 5% to 80% of solvent B over 27 min, followed by an increase to 95% B for 2 min, and returning to 5% B at 29.1 min. The total analysis time was 35 min each for both positive and negative ionization modes. Appendix A lists 59 phytochemicals that were used as reference markers for tentative compound identification.

Identification was achieved by comparing retention times and accurate mass spectra with those of authentic standards where available.

Synthesis and characterization of silver nanoparticles using *N. glauca* extract (NG-AgNPs)

A 10% w/v aqueous extract of *N. glauca*leaves was prepared by maceration in distilled water for 24 h. The solution was then filtered to obtain a clear extract. For nanoparticle synthesis, 9 ml of freshly prepared 0.1 M silver nitrate ($AgNO_3$) solution (0.9 mmol) was placed on a magnetic stirrer, and 1 ml of the *N. glauca* extract was added dropwise under continuous stirring. The pH was maintained between 7 and 9 by adding three drops of concentrated NaOH, which also aided in reducing silver ions.

The mixture was then heated to 40 °C and stirred for 2 h. A gradual color change to brownish-red was observed, indicating the formation of AgNPs. The sample was analyzed by UV-Vis spectrophotometry in the 200–800 nm range, showing a characteristic surface plasmon resonance (SPR) peak at approximately 400–450 nm, confirming nanoparticle formation.

After the synthesis, the nanoparticle suspension was centrifuged at 10,000 rpm for 5 min. The supernatant was removed, and the pellet was redispersed in deionized water to create four formulations (F1–F4). For F1, 10 ml of deionized water was added without stabilizer. For F2, F3, and F4, formulations were prepared with 9 ml of deionized water and 1 ml of PVP solution at 5%, 10%, and 15% concentrations, respectively.

All formulations were probe-sonicated for 50 s at 20% amplitude (10 s pulse-on, 30 s off, repeated until 50 s of total sonication). The samples were stored at 4 °C for 24 h.

After refrigeration, samples were centrifuged again at 10,000 rpm for 30 min. Approximately 5 ml of supernatant was preserved and mixed with each pellet to ensure uniformity. The formulations were then frozen at-80 °C for 24 h and lyophilized for 24 h to obtain NG-AgNPs in powder form for characterization and biological assessment.

Characterization of the prepared NG-AgNPs

UV-Vis spectroscopy confirmed the formation of AgNPs, with a distinct peak at ~440 nm. Dynamic Light Scattering (DLS) was used to measure particle size, zeta potential, and Polydispersity Index (PDI) at 25 °C using a Malvern Zetasizer (NanoZSP model, Malvern Instruments, UK), and a stability study was conducted over 30 days under different storage conditions. Scanning Electron Microscopy (SEM) images of nanoparticle morphology and size were obtained. Samples were prepared by placing a small amount of the nanoparticles on a carbon-coated stub and then sputter-coated with a thin layer of gold to enhance conductivity. The SEM examination was performed using a high-resolution SEM instrument operating at an accelerating voltage of 20 kV. The morphology, size, and surface characteristics of the nanoparticles were captured, and images were taken at various magnifications to ensure a comprehensive analysis.

Antioxidant activity

The antioxidant activities of the four NG-AgNP formulations were determined using the DPPH assay, which measures their ability to reduce the violet DPPH radical to a yellow form, as descriped by Tabana *et al.* (2015) [4]. EC_{50} values (concentration for 50% DPPH scavenging) were determined for each sample.

Serial dilutions (10, 5, 2.5, 1.25, and 0.625% w/v) were prepared for the NG-AgNP formulation (F4) and the crude extract. To 0.2 ml of each dilution, 1.8 ml of DPPH solution (0.002% w/v) was added. The mixtures were kept in the dark for 30 min and the absorbance was measured at 517 nm.

The percent DPPH scavenging was calculated using:

$$\% \text{ Scavenging} = \frac{\text{Abs\_control} - \text{Abs\_sample}}{\text{Abs\_control}} * 100\% \ldots. (2)$$

Where Abs_control is the absorbance of DPPH without the sample, and Abs_sample is the absorbance of the sample.

Antibacterial activity of NG-AgNPs

The antibacterial activity of the biosynthesized NG-AgNPs was evaluated using the Kirby-Bauer well diffusion assay according to Clinical and Laboratory Standards Institute (CLSI) guidelines (2020) [17]. The assay was performed using *Staphylococcus aureus* (ATCC 29213) as a g-positive model and *Pseudomonas aeruginosa* (ATCC 27853) as a g-negative model. Wells of 6 mm diameter were created in agar plates and filled with NG-AgNPs, $AgNO_3$, or crude extract. The plates were incubated at 37 °C for 24 h, and the diameters of the inhibition zones were measured. For comparison, standard antibiotics (vancomycin, doxycycline, tetracycline, azithromycin, ciprofloxacin, clarithromycin, and amoxicillin) were tested similarly.

The Minimum Inhibitory Concentration (MIC) was determined in 96-well plates using two-fold serial dilutions of NG-AgNPs, crude extract, $AgNO_3$, and doxycycline (control) with the bacterial inocula. After overnight incubation, the MIC was the lowest concentration with no visible growth. All experiments were performed in triplicate (n = 3 independent biological replicates), and the results are presented as mean±standard deviation (SD).

Anticancer activity

The anticancer activity of the best formulation (F4) and crude extract was assessed by MTT assay on three cancer cell lines, A549 (lung), HT-29 (colorectal), MCF-7 (breast), and a normal endothelial cell line (EA. hy926) as a control.

The cells were cultured in DMEM (EA. hy926) or RPMI-1640 (A549, HT-29, and MCF-7). Different concentrations of NG-AgNPs and crude extracts (1000–7.81 µg/ml) were used. The cells were incubated for 48 h at 37 °C with 5% CO_2. The IC_{50} for each treatment (concentration causing 50% growth inhibition) was determined, indicating cytotoxic potency.

Cytotoxicity assays were performed in 96-well plates with cells seeded in triplicate for each concentration. Each experiment was independently repeated three times (n = 3). Cell viability was expressed as mean±SD of three independent experiments.

Statistical analysis

Zones of inhibition were recorded in millimeters (mm) and expressed as mean±SD (n = 3 per treatment). For each bacterium, treatments were compared using one-way ANOVA (ordinary) followed by Tukey–Kramer multiple comparisons. Assumptions were checked (normality of residuals and Brown–Forsythe test for homogeneity of variances). Given balanced sample count (n) and small standard deviation (SDs), ANOVA was considered robust. $\alpha = 0.05$. All analyses were performed in GraphPad Prism, version 10 (GraphPad Software, San Diego, CA, USA).

RESULTS

Extraction percentage yield %

The extraction yields varied across solvents and methods. The Water-Soxhlet, Water-Maceration, Ethanol-Maceration, and Ethanol-Soxhlet yields were 41.26, 34.8, 16.14, and 6.7%, respectively. The highest TPC was observed in the Ethanol-Soxhlet extract (484±1.3 mg GAE/g dry extract), followed by the Ethanol-Maceration extract (472.4±0.9 mg GAE/g). The Water-Soxhlet extract showed 165.2±0.2 mg GAE/g, and the Water-Maceration extract had 144.9±0.16 mg GAE/g. TFC showed a similar trend: the highest was in the ethanol Soxhlet extract (274.9±1.2 mg QE/g dry extract), followed by Ethanol-Maceration (209±2.5 mg QE/g). The Water-Soxhletextract (80 ml) had 117.8±0.73 mg QE/g, and Water-Macerationhad 99.1±0.1 mg QE/g. The higher phenolic and flavonoid content of the ethanolic extracts can be attributed to the ability of ethanol to dissolve a broad range of compounds, enhancing the extraction of polyphenols and flavonoids. Heat and continuous solvent recycling in Soxhlet likely further improves the extraction efficiency. Thus, Ethanol-Soxhlet yielded more phenolic and flavonoid compounds than water extractions.

Liquid chromatography–mass spectrometry (LC-MS) analysis

Extraction ion chromatography (EIC) – positive mode

Several compounds were identified: Catechol (retention time, RT 3.06 min; intensity increased from 0 in blank to 2026 in sample),

hydrocinnamic acid (RT 8.41 min; intensity 1128 vs 340 blank), umbelliferone (RT 3.69), p-coumaric acid (RT 4.59), and 4-methylumbelliferone (7.42 min; detectable in the blank at 40,396, but markedly higher in the sample at 191,984, suggesting true presence despite background interference in the blank).

Extraction ion chromatography (EIC) – negative mode

The identified compounds included gallic acid (RT 3.36 min; intensity (46,412 vs. 334 blank), (-)-quinic acid (RT 1.93 min; 4666 vs. 0 blank), 2-(4-methylphenyl)-2-propanol (RT 4.5 min; 4314 vs. 154 blank), oleic acid (RT 14.28 min; 3174 vs. 1924 blank), (E)-2-octenal (RT 5.5 min; 1192 vs. 152 blank), and (-)-α-fenchyl acetate (RT 7.76 min; 1044 vs. 0 blank). Fig. 1,2 and Appendix B1 and B2 list the positive-and negative-mode results, respectively.

Preparation of NG-AgNPs

The water maceration extract was slightly yellow; after adding $AgNO_3$ and adjusting the pH with NaOH, the solution turned brown (fig. 3). After one hour, the color intensity increased, confirming Ag^+ reduction and NG-AgNP formation [18].

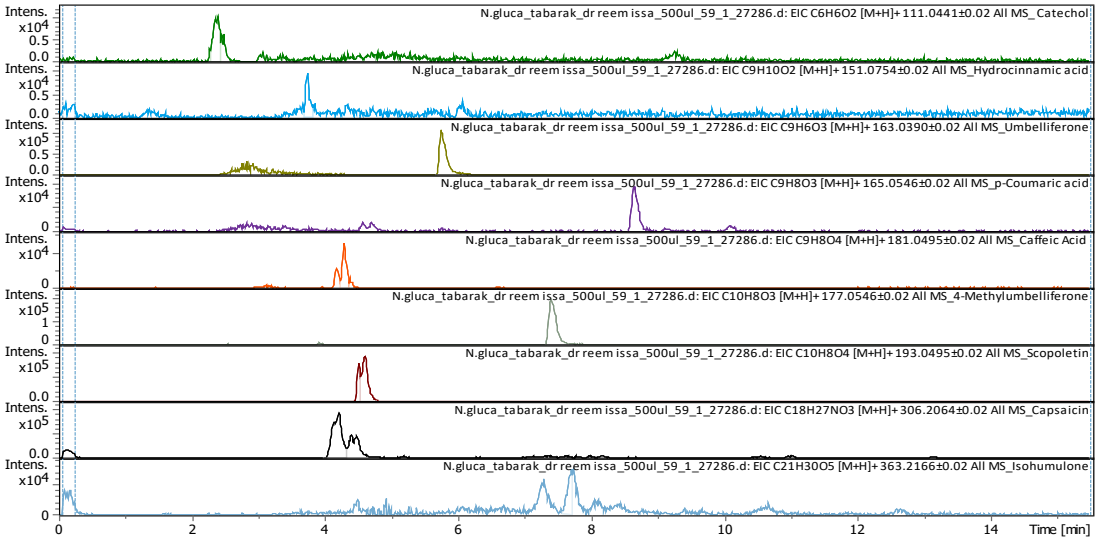

Fig. 1: The results of the EIC-positive mode and the compounds found in *N. glauca* extract

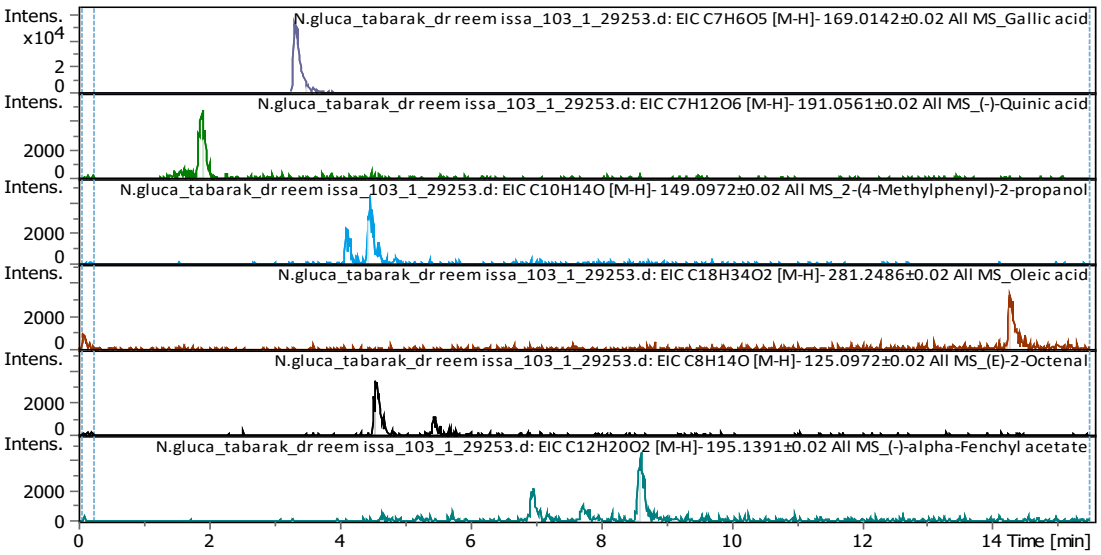

Fig. 2: The results of EIC-negative mode and the compounds found in *N. glauca* extract

Characterization of the prepared NG-AgNPs

Ultraviolet-visible (UV-Vis) spectroscopy

The NG-AgNPs showed a characteristic peak at 440.50 nm, indicating successful nanoparticle formation.

Scanning electron microscopy (SEM)

SEM analysis showed that the NG-AgNPs were roughly spherical with particle sizes of 188–280 nm, which is consistent with the DLS results. Fig. 4 shows SEM images of NG-AgNPs (F4).

Dynamic light scattering (DLS) and stability

The stability of NG-AgNPs was evaluated in terms of zeta potential, particle size, and polydispersity index (PDI) under storage at room temperature and in a refrigerator over 30 days, as shown in fig. 5 (1–3). F1 had the best initial zeta potential (-29.6 mV) and remained stable under all conditions. The formulations with PVP (F2–F4) had slightly lower negative surface charges (-16.5 to-18.7 mV). All formulations were stable at room temperature and in refrigerator. For particle size stability, F1 (initial 151 nm) grew to micron size within 20–30 days. F2 and F4 were unexpectedly stable at 40 ℃, yielding the

lowest particle sizes after 30 days (173 and 124 nm, respectively). Storage at room temperature and 4 °C also resulted in acceptable particle size stability for F2 and F4, with only a slight increase. F3 was the most stable at 4 °C (145.6 nm at 30 days). The initial PDI of F1 was high (0.753), reaching 1 after 20 days. F4 had the lowest initial PDI (0.216) and stayed<0.3 under all conditions. F2 and F3 showed less stability, with PDI>0.3 after 10 days under all conditions. F4 was the most stable in terms of its size, zeta potential, and PDI.

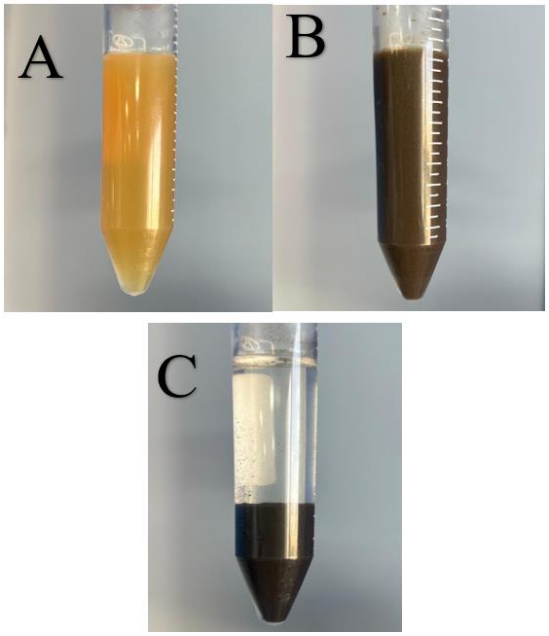

Fig. 3: Water-maceration extract (A) before and (B) after the addition of sodium hydroxide (NaOH) solution, and (C) after one-hour stand

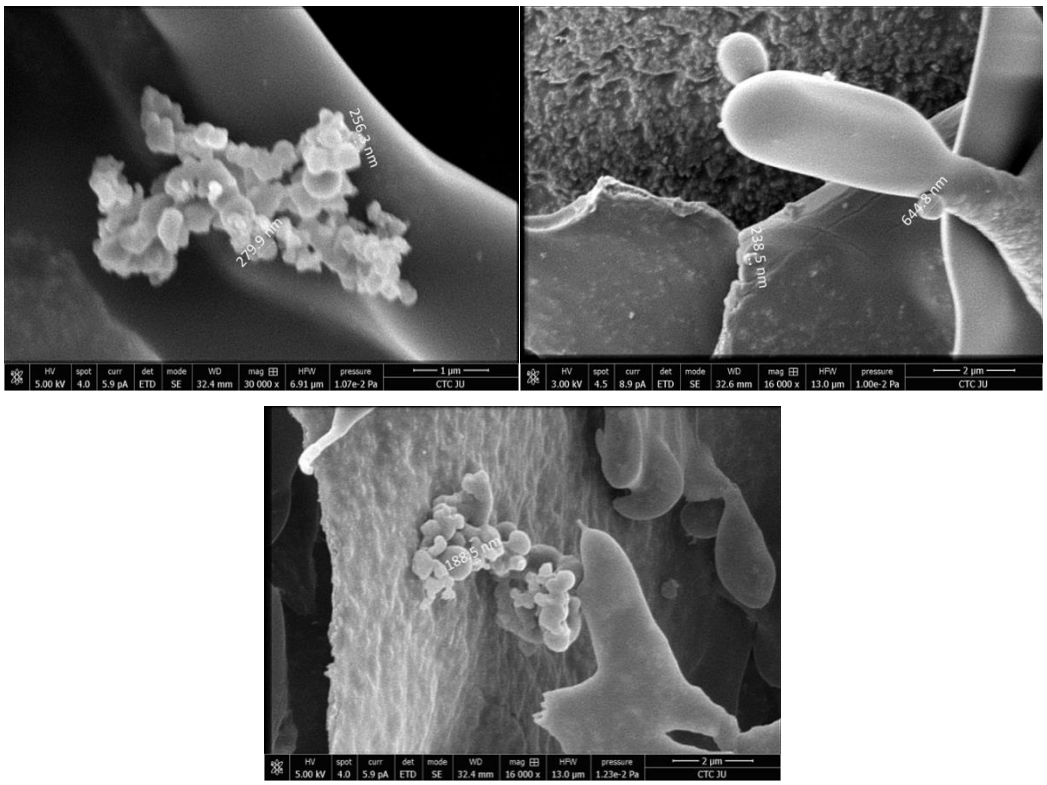

Fig. 4: SEM images of the prepared NG-AgNPs (formulation F4)

Determination of antioxidant activity (DPPH assay)

The ethanolic Soxhlet extract exhibited the highest antioxidant activity (EC_{50} = 0.0606% w/v). NG-AgNPs showed moderate antioxidant activity (EC_{50} = 1.348% w/v). The water-maceration extract EC_{50} was 1.522% (slightly less effective than that of NG-AgNPs). Soxhlet-water extract $EC_{50}$was 1.816% w/v (moderate). The maceration ethanol extract exhibited the lowest antioxidant activity (EC_{50} = 2.234% w/v). Vitamin C (positive control) was highly potent (EC_{50} = 0.000159%, w/v). These results suggest that the Soxhlet-

ethanol extract had the strongest DPPH scavenging activity and that maceration-ethanol was the weakest among the tested samples. NG-AgNPs had moderate activity, comparable to that of the water-maceration extract but less than that of the Soxhlet-ethanol extract.

Determination of antibacterial activity (Kirby-bauer assay)

Staphylococcus aureus

NG-AgNPs produced inhibition zones of 24.6±0.3 at 0.5% w/v, 21.6±0.1 at 0.125% w/v, and 20.3±0.2 at 0.062% w/v; the crude extract (10% w/v) reached 18.0±0.1. Standard antibiotics produced: vancomycin 18.0±0.2, doxycycline 25.0±0.5, tetracycline 27.0±0.9, azithromycin 22.0±0.2, and ciprofloxacin 21.0±0.2.

A one-way ANOVA across treatments was significant ($F(8, 18) = 196.32$, $p<0.0001$). Tukey's post hoc showed NG-AgNPs 0.5% was greater than the crude extract ($p<0.0001$), greater than vancomycin ($p<0.0001$), greater than azithromycin ($p<0.0001$) and ciprofloxacin ($p<0.0001$); not different from doxycycline ($p = 0.925$); and lower than tetracycline ($p<0.0001$)."

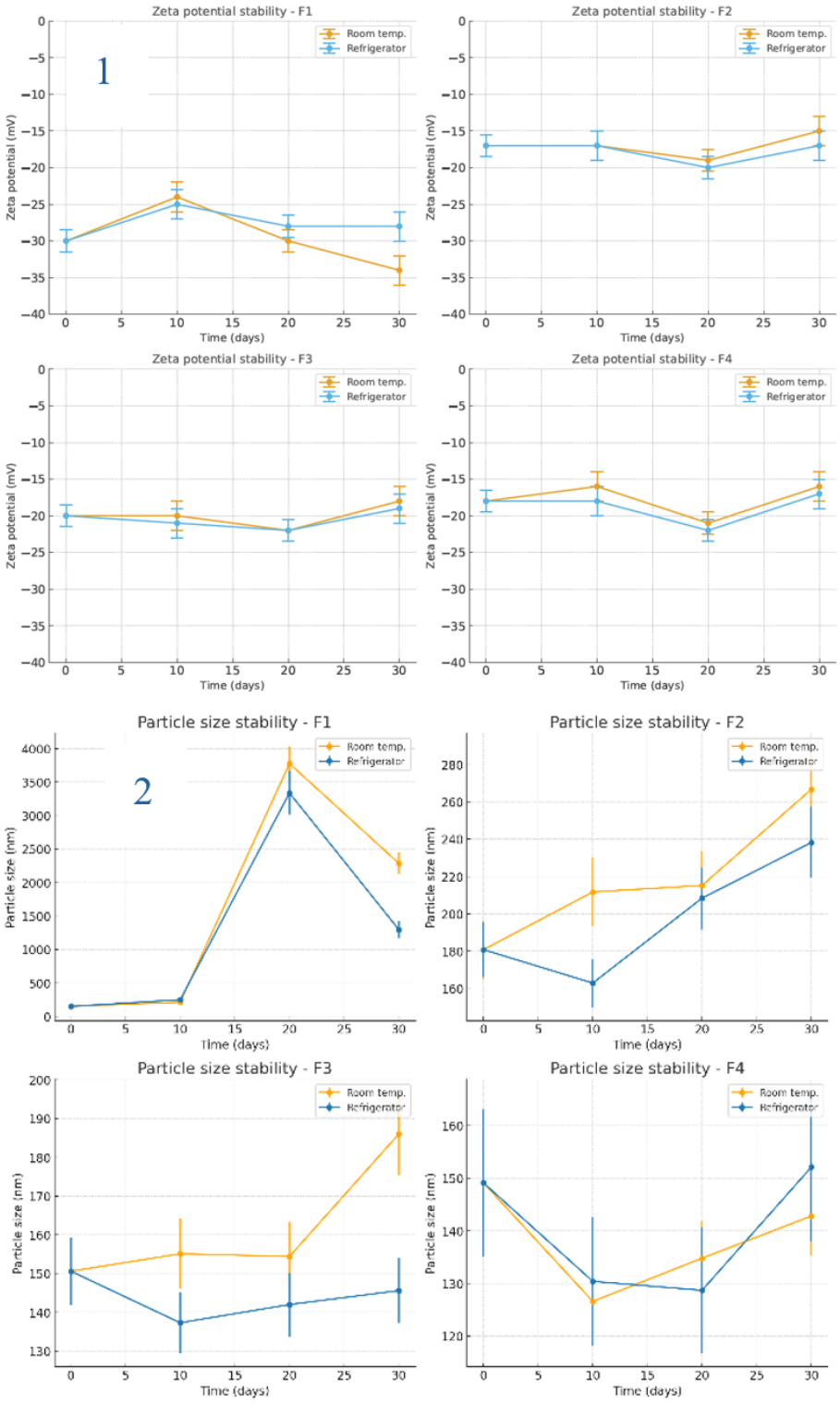

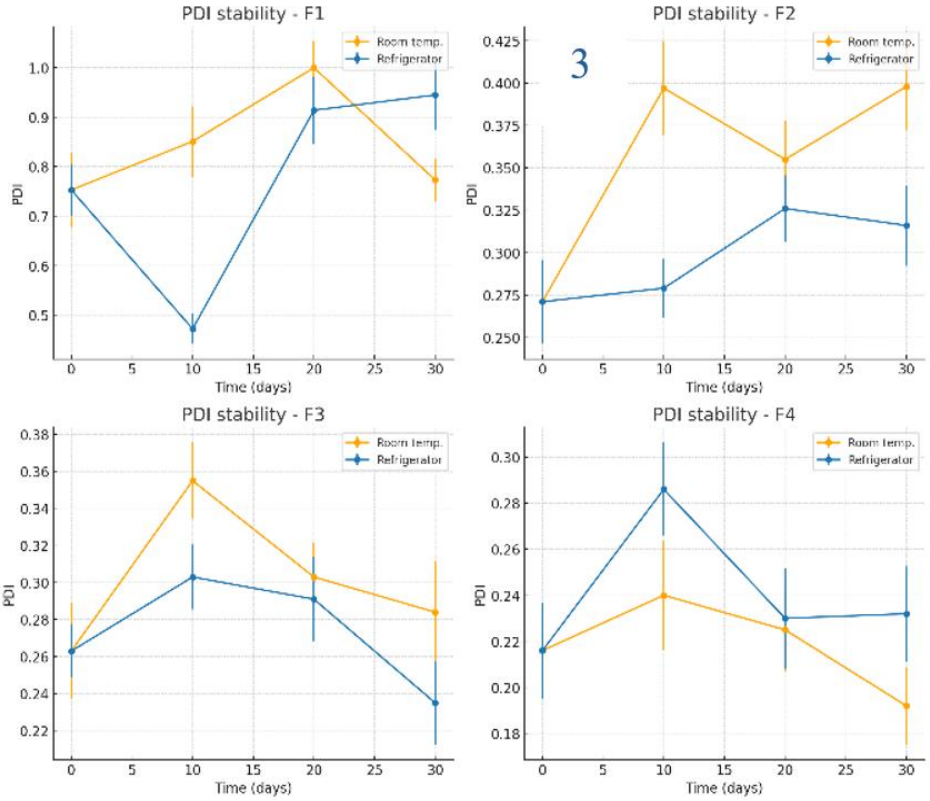

Fig. 5: Stability evaluation of NG-AgNPs: (1) Zeta potential, (2) Particle size, and (3) PDI of silver nanoparticles prepared using *N. glauca* extract. Data are reported as mean±SD (n = 3 independent measurements per time point)

Pseudomonas aeruginosa

NG-AgNPs (0.5% w/v) produced 20.6±0.2; the crude extract showed 0.0±0.0. Antibiotics yielded: clarithromycin 21.0±0.2, doxycycline 9.0±0.4, tetracycline 22.0±1.0, amoxicillin 0.0±0.0, and ciprofloxacin 31.0±0.6.

A one-way ANOVA across treatments was significant ($F(6, 14) = 2029.24$, $p<0.0001$). Tukey's post hoc indicated NG-AgNPs 0.5% was greater than the crude extract ($p<0.0001$), greater than amoxicillin ($p<0.0001$) and doxycycline ($p<0.0001$); not different from clarithromycin ($p = 0.928$); and lower than tetracycline ($p = 0.028$) and ciprofloxacin ($p<0.0001$)."

Taken together, NG-AgNPs significantly outperformed the crude plant extract and were statistically comparable to certain standard antibiotics (e. g., doxycycline for *S. aureus*; clarithromycin for *P. aeruginosa*), underscoring that a plant-derived nanoformulation-without known resistance mechanisms—can match established antibiotics against these strains.

Determination of minimum inhibitory concentration (MIC)

For *S. aureus*, the crude extract had no detectable MIC (no inhibition even at the highest concentration), indicating no effective antibacterial action. NG-AgNPs showed an MIC between wells 5 and 6 (dilution 1:16–1:32 of 5 mg/ml), indicating much greater potency than the crude extract. $AgNO_3$ had an MIC between wells 2 and 3 (dilution 1:2–1:4), reflecting lower effectiveness compared to NG-AgNPs. Doxycycline (positive control) completely inhibited cell growth in wells 7 and 8. For *P. aeruginosa*, the crude extract of *P. aeruginosa* showed no MIC at the highest concentration (consistent with Kirby-Bauer results showing no activity). NG-AgNPs grew only between wells 4 and 5 (dilution 1:8–1:16 of 5 mg/ml), indicating a higher potency against *P. aeruginosa* than the crude extract. $AgNO_3$ showed complete inhibition at a lower dilution (more concentrated) than NG-AgNPs, meaning NG-AgNPs were more potent. Doxycycline showed weak activity (MIC between Wells 2 and 3).

Anticancer activity of the prepared NG-AgNPs

For the HT-29 colorectal cells, the crude extract IC_{50} was 450.2±13.4 µg/ml (low cytotoxicity), whereas NG-AgNPs IC_{50} was 2.517±0.221 µg/ml, indicating much higher cytotoxicity against HT-29. For A549 lung cells, crude extract IC_{50} was 378.7±10.5 µg/ml, vs NG-AgNPs 25.11±0.19 µg/ml, showing NG-AgNPs are significantly more potent. For MCF-7 breast cells, the crude extract did not reach the IC_{50} at the tested concentrations, suggesting insufficient potency. NG-AgNPs had an IC_{50} 24.53±0.71 µg/ml, indicating a strong effect on MCF-7 cells. For the normal EA. hy926 endothelial cells, crude extract IC_{50} was 16.88±0.04 µg/ml (some toxicity to normal cells), whereas NG-AgNPs did not reach an IC_{50} at the highest concentration tested (1000 µg/ml), indicating significantly lower toxicity.

Table 1: MIC values of various treatments against *P. aeruginosa* and *S. aureus*

Treatment	*P. aeruginosa* MIC (mg/ml)	*S. aureus* MIC (mg/ml)
Water-maceration extract	R (no MIC)	R (no MIC)
NG-AgNPs	0.625–0.312	0.312–0.156
$AgNO_3$	34–17	34–17
Doxycycline (control)	25–12.5	0.781–0.400

R = resistant (no inhibition at highest concentration tested).

Table 2: IC_{50} values (n=3) of crude extract and NG-AgNPs on various cancer and normal cell lines (MTT assay)

Treatment	HT-29 (µg/ml)	A549 (µg/ml)	MCF-7 (µg/ml)	EA. hy926 (µg/ml)
Crude extract	450.2±13.4	378.7±10.5	>1000 (No IC_{50})	16.88±0.04
NG-AgNPs (F4)	2.517±0.221	25.11±0.19	24.53±0.71	>1000 (No IC_{50})

Data are reported as mean±SD (n = 3 independent measurements per cell line).

DISCUSSION

This study successfully synthesized green silver nanoparticles (AgNPs) using a natural extract and demonstrated their multifaceted bioactivity. We found that the optimized nanoparticle formulation (designated *F4*) was physically stable and well-characterized, with a small size and strong negative surface charge. Biologically, the ethanolic Soxhlet extract of *N. glauca* exhibited the highest antioxidant capacity, while the NG-AgNP formulation showed moderate antioxidant activity. In contrast, NG-AgNPs displayed superior antibacterial efficacy, outperforming the crude extract with a similar activity to antibiotic controls. The AgNPs also showed promising anticancer effects, with selective toxicity toward cancer cells over normal cells. These findings highlight the synergistic advantages of combining silver nanoparticles with phytochemicals, improving the delivery and potency of bioactive compounds in antimicrobial and anticancer applications.

The green-synthesized AgNP formulation (F4) was found to be stable and uniformly nanosized. Dynamic light scattering and electron microscopy revealed spherical nanoparticles with an average diameter in the tens of nanometers, confirming successful formation of colloidal silver. Importantly, formulation F4 remained stable with minimal aggregation over time, attributable to the presence of polyvinylpyrrolidone (PVP) as a capping agent. PVP binds to the AgNP surface via its carbonyl and amine groups, creating a protective coating. This PVP cappingprovides steric hindrance and prevents particle agglomeration, thereby significantly enhancing colloidal stability [19]. In our formulation, the zeta potential was highly negative, indicating a well-dispersed and stable suspension. Generally, nanoparticle suspensions with zeta potentials above ±30 mV are considered stable due to strong repulsive forces [20]. The high absolute zeta potential of F4 likewise reflects excellent stability conferred by both PVP and negatively charged phytochemicals adsorbed on the AgNP surface. Our selected formulation (F4) shows a DLS hydrodynamic diameter<150 nm and a moderately negative ζ (≈−16 to −19 mV). This sits well within typical ranges for green/bio-stabilized AgNPs, where most reports are<200 nm with negative surface charge from plant/polymer capping. For example, *Brassica carinata* microgreen AgNPs reported a DLS size of 196.4±2.1 nm and ζ = −22.5±1.2 mV [21]; *Turbinaria ornata*–mediated AgNPs showed 128.3 nm by DLS with ζ = −63.3 mV [22]; and microalga-broth AgNPs spanned ∼64–128 nm with ζ between −22 and −37 mV [23]. Together, these place our F4 (<150 nm, negatively charged) in accordance with the prevailing literature (<200 nm, negative ζ). These comparable results validate our synthesis approach and suggest the F4 nanoparticles are suitable for biological applications, where small size and stable dispersity are crucial for bioavailability and cellular uptake.

In antioxidant assays, the ethanol-Soxhlet extract showed the strongest free-radical scavenging activity among the tested samples. This extract's superior performance is likely due to its high content of phenolic and flavonoid compounds, which are well-known to donate hydrogen atoms or electrons to neutralize free radicals. Indeed, the total phenolic and flavonoid content (TPC/TFC) of the crude extract is expected to be high, correlating directly with its antioxidant potency [24]. By contrast, the AgNP formulation exhibited only moderate antioxidant activity. The reduction in antioxidant efficacy for NG-AgNPs can be explained by the utilization and immobilization of some phytochemicals during nanoparticle synthesis. Many phenolics are consumed as reducing agents to convert $Ag^+$to Ag and remain bound to the nanoparticle surface as capping agents [25]. Consequently, fewer free phytochemicals are available in solution to directly scavenge radicals compared to the bulk extract. Nonetheless, the NG-AgNPs did retain measurable antioxidant capacity, implying that some antioxidant constituents are still present on the nanoparticle surface or within its corona. These results align with the notion that phenolic-capped AgNPs owe their antioxidant ability to the plant-derived compounds attached to them. Our findings underscore that while green-synthesized AgNPs carry over some antioxidant functionality, the uncapped extract in free form is more efficacious in antioxidant assays due to the greater availability of active phytochemicals.

The antibacterial tests revealed that the green-synthesized NG-AgNPs had potent activity against both Gram-positive *S. aureus* and Gram-negative *P. aeruginosa*. Notably, the NG-AgNPs produced larger zones of inhibition compared to the crude extract alone, and even outperformed standard silver nitrate ($AgNO_3$) solution and certain antibiotics in our assays. Such results highlight a synergistic antibacterial effect arising from the combination of AgNPs with bioactive phytochemicals from the extract. Similar observations have been reported with other plant-based AgNPs, which showed significantly greater antimicrobial activity than either the plant extract or $AgNO_3$ alone [26, 27]. The enhanced efficacy can be attributed to multiple mechanisms. Silver nanoparticles are well-known to disrupt microbial cells by attaching to the cell wall and membrane, increasing permeability, and then penetrating inside to damage biomolecules. They release Ag^+ions that generate reactive oxygen species (ROS) and induce oxidative stress, leading to protein and DNA damage in microbes [28]. In our formulation, the phytochemical capping agents likely augment these effects. Many plant metabolites (e. g. polyphenols, flavonoids) have inherent antimicrobial properties, such as compromising bacterial membranes or interfering with metabolic enzymes. When bound to AgNPs, these phytochemicals can facilitate better adhesion of NPs to bacterial cells or provide additional routes of toxicity, they might also independently disrupt cell membrane integrity or function as efflux pump inhibitors, thereby sensitizing bacteria to silver's action. Gram-negative *P. aeruginosa*, normally resistant to many agents, was effectively inhibited by NG-AgNPs – whereas the botanical extract alone was ineffective – illustrating that the nanoformulation overcame the permeability barrier of the Gram-negative outer membrane. Literature suggests that flavonoid-capped AgNPs can indeed penetrate bacterial biofilms and cell envelopes more efficiently, leveraging both the nanoparticle's physical interactions and the phytochemicals' bioactivity [28, 29]. Thus, our green AgNPs leverage both the metallic core and the organic coat to achieve broad-spectrum antibacterial activity. This finding is significant for developing nanobiotic strategies, as the NG-AgNPs could potentially reduce the required dose of silver while extending antimicrobial efficacy against resistant pathogens.

The green-synthesized AgNPs also demonstrated promising anticancer effects, with evidence of selective cytotoxicity towards cancer cells. In cell culture experiments, the NG-AgNPs induced higher death rates in cancer cell lines compared to treatments with the crude extract or to untreated controls, while showing no toxicity in normal cell line. This preferential cytotoxicity suggests that the nanoformulation can more specifically target malignant cells. One plausible explanation is that cancer cells, due to their rapid division and altered metabolism, tend to uptake nanoparticles more readily than normal cells [30]. Differences in cell membrane composition and the enhanced endocytic activity of cancer cells allow greater internalization of AgNPs, leading to higher intracellular silver and phytochemical concentrations in tumor cells [30]. Additionally, if applied *in vivo*, the size of our AgNPs falls in a range that could exploit the Enhanced Permeability and Retention (EPR) effect – leaky tumor vasculature allows nanoparticles to accumulate in tumor tissue more than in healthy tissue [31]. This passive targeting, combined with potentially active targeting from surface

phytochemicals, would further improve delivery to cancer cells and spare normal cells. The crude extract is rich in cembranoid diterpenes, compounds which have shown cytotoxic and pro-apoptotic effects against cancer in previous studies [32]. The LC-MS analysis confirmed the presence of such terpenoids alongside other metabolites in the extract, suggesting that these could be partly responsible for the observed anti-proliferative activity. By formulating them into nanoparticles, their bioavailability and cellular uptake might be enhanced, as hydrophobic diterpenes can hitch a ride on the nanoparticle into cells. Similarly, Umbelliferone (7-hydroxycoumarin) and hydrocinnamic acid derivatives were identified in the extract (per LC-MS data), and these phytochemicals are known for diverse bioactivities, including antioxidant and anticancer effects [33]. Although each compound alone may exert only moderate effects, in concert and delivered via AgNPs, they can produce a combined cytotoxic impact on cancer cells. This is supported by reports that green-fabricated AgNPs often achieve greater cancer cell killing than the free phytochemical extract, due to improved cellular uptake and sustained release of bioactive agents [34]. Our results concur with those trends: the NG-AgNPs showed higher efficacy against cancer cells than the crude extract, underlining the benefit of the nano-delivery system.

Phytochemical profiling (LC-MS) of the extract revealed numerous secondary metabolites that likely contributed to the biological activities observed. Key compounds tentatively identified include phenolic acids (such as hydrocinnamic acid), coumarins (such as umbelliferone), and terpenoids (including cembranoid diterpenes as noted above). Each of these classes has reported bioactivity: for instance, coumarins like umbelliferone exhibit antioxidant and anti-inflammatory properties and have shown anticancer potential by inducing apoptosis in tumor cells [35]. Phenolic acids are well known for their free-radical scavenging ability and can also impair microbial growth by damaging membranes or enzymes. Cembranoid diterpenes, commonly found in certain plants and marine organisms, are documented to possess anti-inflammatory and anti-cancer effects [32]. The co-presence of these diverse phytochemicals on the AgNP surface means the nanoparticles function as a delivery vehicle for a cocktail of bioactive agents. This likely explains the breadth of activity (antioxidant, antibacterial, anticancer) displayed by NG-AgNPs. The phytochemicals not only reduced and stabilized the nanoparticles during synthesis but also remained bound as a bioorganic corona that interacts with biological targets. We propose that this synergistic interplay – silver nanoparticles acting in tandem with capping phytochemicals – is responsible for the enhanced antibacterial and cytotoxic effects observed. Such synergy is supported by other studies on green-synthesized AgNPs, where the combination of metal ions with plant metabolites produced more potent bioactivity than either component alone [26, 27]. In summary, the identified compounds (hydrocinnamic acid, umbelliferone, cembranoid terpenes, etc.) form an integral part of the NG-AgNPs' mode of action, each contributing to the overall efficacy through their known mechanisms while being delivered more effectively to targets via the nanoparticle matrix.

FUTURE PERSPECTIVES

To translate these findings into practical biomedical applications, further studies are warranted. In-depth *in vivo* evaluations should be conducted to verify the Enhanced Permeability and Retention effect and therapeutic index of NG-AgNPs in animal tumor models and infection models. Chronic toxicity and biocompatibility assessments will be essential to ensure safety. Additionally, optimization of the nanoformulation could be explored – for instance, adjusting particle size, surface coatings, or conjugating targeting ligands – to maximize delivery to tumor tissues or infection sites. Isolation and characterization of the most active phytochemical ingredients (such as specific diterpenes or coumarins) might allow the design of nano-delivery systems for those purified compounds, further improving efficacy and consistency. By building on the current findings, future research can advance these green-synthesized AgNPs toward clinical or pharmaceutical development. Overall, our study highlights a compelling approach to integrate natural product chemistry with nanotechnology, yielding a synergistic therapeutic platform that addresses multiple biomedical challenges.

CONCLUSION

In conclusion, we have developed a PVP-stabilized, phytochemical-capped silver nanoparticle formulation that harnesses the therapeutic potentials of both silver and natural product compounds. The formulated NG-AgNPs demonstrated robust antioxidant, antibacterial, and anticancer activities, with clear advantages over the crude extract or silver salt alone. The results underscore the value of green synthesis in creating nanomaterials that are not only stable and well-sized but also biologically potent due to the incorporated phytochemicals. This work positions the NG-AgNPs as a promising multifunctional agent for potential applications in infection control and cancer therapy, especially given their selective toxicity towards cancer cells and efficacy against antibiotic-resistant bacteria.

FUNDING

Nil

AUTHORS CONTRIBUTIONS

Conceptualization, T. R. A.; methodology, T. R. A.; validation, R. I. and S. M.; formal analysis, T. R. A.; investigation, T. R. A.; resources, R. I. and S. M.; data curation, T. R. A.; writing—original draft preparation, T. R. A.; writing—review and editing, R. I. and S. M.; visualization, T. R. A.; supervision, R. I. and S. M.; project administration, R. I. and S. M. All authors have read and agreed to the published version of the manuscript.

CONFLICTS OF INTERESTS

The authors declare no conflicts of interest

REFERENCES

1. Furer V, Hersch M, Silvetzki N, Breuer GS, Zevin S. Nicotiana glauca (tree tobacco) intoxication two cases in one family. J Med Toxicol. 2011 Mar;7(1):47-51. doi: 10.1007/s13181-010-0102-x, PMID 20652661.
2. Janakat S, Al-Merie H. Evaluation of hepatoprotective effect of Pistacia lentiscus Phillyrea latifolia and Nicotiana glauca. J Ethnopharmacol. 2002 Nov 1;83(1-2):135-8. doi: 10.1016/S0378-8741(02)00241-6, PMID 12413719.
3. Zou X, BK A, Abu Izneid T, Aziz A, Devnath P, Rauf A. Current advances of functional phytochemicals in Nicotiana plant and related potential value of tobacco processing waste: a review. Biomed Pharmacother. 2021 Nov 1;143:112191. doi: 10.1016/j.biopha.2021.112191, PMID 34562769.
4. Tabana YM, Dahham SS, Ahmed Hassan LE, Al-Mansoub MA, Taleb-Agha M, Abdul Majid AM. *In vitro* anti-metastatic and antioxidant activity of Nicotiana glauca fraction against breast cancer cells. Adv Biol Res. 2015;9(2):95-102. doi: 10.5829/idosi.abr.2015.9.2.9521.
5. Jassbi AR, Zare S, Asadollahi M, Schuman MC. Ecological roles and biological activities of specialized metabolites from the genus Nicotiana. Chem Rev. 2017 Oct 11;117(19):12227-80. doi: 10.1021/acs.chemrev.7b00001, PMID 28960061.
6. Tabana Y. Anti-tumor study of scopoletin and rubbing-mercapto-nitrile from Nicotiana glauca [dissertation]. Penang, Malaysia: Universiti Sains Malaysia; 2016.
7. Ali Alghamdi AA. Phytoconstituents screening and antimicrobial activity of the invasive species Nicotiana glauca collected from Al-Baha region of Saudi Arabia. Saudi J Biol Sci. 2021 Mar 1;28(3):1544-7. doi: 10.1016/j.sjbs.2020.12.034, PMID 33732038.
8. Abass Sofi M, Sunitha S, Ashaq Sofi M, Khadheer Pasha SK, Choi D. An overview of antimicrobial and anticancer potential of silver nanoparticles. J King Saud Univ Sci. 2022 Feb 1;34(2):101791. doi: 10.1016/j.jksus.2021.101791.
9. Ijaz I, Gilani E, Nazir A, Bukhari A. Detail review on chemical, physical and green synthesis classification, characterizations and applications of nanoparticles. Green Chem Lett Rev. 2020 Jul 2;13(3):223-45. doi: 10.1080/17518253.2020.1802517.
10. Srivastava S, Usmani Z, Atanasov AG, Singh VK, Singh NP, Abdel Azeem AM. Biological nanofactories: using living forms for metal nanoparticle synthesis. Mini Rev Med Chem. 2021 Feb

1;21(2):245-65. doi: 10.2174/1389557520999201116163012, PMID 33198616.

11. Tripathi N, Goshisht MK. Recent advances and mechanistic insights into antibacterial activity antibiofilm activity and cytotoxicity of silver nanoparticles. ACS Appl Bio Mater. 2022 Mar 31;5(4):1391-463. doi: 10.1021/acsabm.2c00014, PMID 35358388.
12. Kumar H, Bhardwaj K, Nepovimova E, Kuca K, Dhanjal DS, Bhardwaj S. Antioxidant functionalized nanoparticles: a combat against oxidative stress. Nanomaterials (Basel). 2020 Jul 8;10(7):1334. doi: 10.3390/nano10071334, PMID 32650608.
13. Jain AS, Pawar PS, Sarkar A, Junnuthula V, Dyawanapelly S. Bionanofactories for green synthesis of silver nanoparticles: toward antimicrobial applications. Int J Mol Sci. 2021 Nov 5;22(21):11993. doi: 10.3390/ijms222111993, PMID 34769419.
14. Habib MA, Islam MM, Islam MM, Hasan MM, Baek KH. Current status and de novo synthesis of anti-tumor alkaloids in Nicotiana. Metabolites. 2023 Apr 30;13(5):623. doi: 10.3390/metabo13050623, PMID 37233664.
15. Lawag IL, Nolden ES, Schaper AA, Lim LY, Locher C. A modified folin–ciocalteu assay for the determination of total phenolics content in honey. Appl Sci. 2023;13(4):2135. doi: 10.3390/app13042135.
16. Tristantini D, Amalia R. Quercetin concentration and total flavonoid content of anti-atherosclerotic herbs using aluminum chloride colorimetric assay. AIP Conf Proc. 2019 Dec 10;2193(1):030012. doi: 10.1063/1.5139349.
17. Clinical and Laboratory Standards Institute (CLSI). Performance standards for antimicrobial susceptibility testing. 22nd informational supplement. Wayne (PA): CLSI; 2012.
18. Gloria EC, Ederley V, Gladis M, Cesar H, Jaime O, Oscar A. Synthesis of silver nanoparticles (AgNPs) with antibacterial activity. J Phys: Conf Ser. 2017 Jun 1;850(1):012023. doi: 10.1088/1742-6596/850/1/012023.
19. Zein R, Alghoraibi I, Soukkarieh C, Ismail MT, Alahmad A. Influence of polyvinylpyrrolidone concentration on properties and anti-bacterial activity of green synthesized silver nanoparticles. Micromachines (Basel). 2022;13(5):777. doi: 10.3390/mi13050777, PMID 35630244.
20. Tamma MA, Nsairat H, El-Tanani M, Madi R. *In vitro* evaluation of lipidic nanocarriers for mebendazole delivery to improve anticancer activity. Drug Dev Ind Pharm. 2024 Nov 1;50(11):917-26. doi: 10.1080/03639045.2024.2428405, PMID 39527027.
21. Somda D, Bargul JL, Wesonga JM, Wachira SW. Green synthesis of Brassica carinata microgreen silver nanoparticles characterization safety assessment and antimicrobial activities. Sci Rep. 2024;14(1):29273. doi: 10.1038/s41598-024-80528-6, PMID 39587236.
22. Raj CT, Muthukumar K, Dahms HU, James RA, Kandaswamy S. Structural characterization antioxidant and anti-uropathogenic potential of biogenic silver nanoparticles using brown seaweed Turbinaria ornata. Front Microbiol. 2023;14:1072043. doi: 10.3389/fmicb.2023.1072043, PMID 37727290.
23. Pernas Pleite C, Conejo Martinez AM, Fernandez Freire PF, Hazen MJ, Marin I, Abad JP. Microalga broths synthesize antibacterial and non-cytotoxic silver nanoparticles showing synergy with antibiotics and bacterial ROS induction and can be reused for successive AgNP batches. Int J Mol Sci. 2023;24(22):16183. doi: 10.3390/ijms242216183, PMID 38003373.
24. Elmastas M, Telci I, Aksit H, Erenler R. Comparison of total phenolic contents and antioxidant capacities in mint genotypes used as spices / Baharat olarak kullanılan nane genotiplerinin toplam fenolik icerikleri ve antioksidan kapasitelerinin karsılastırılması. Turk J Biochem. 2015;40(6):456-62. doi: 10.1515/tjb-2015-0034.
25. Bedlovicova Z, Strapac I, Balaz M, Salayova A. A brief overview on antioxidant activity determination of silver nanoparticles. Molecules. 2020 Jul 15;25(14):3191. doi: 10.3390/molecules25143191, PMID 32668682.
26. Singh R, Hano C, Nath G, Sharma B. Green biosynthesis of silver nanoparticles using leaf extract of *Carissa carandas L.* and their antioxidant and antimicrobial activity against human pathogenic bacteria. Biomolecules. 2021 Feb 9;11(2):299. doi: 10.3390/biom11020299, PMID 33671333.
27. Abdel-Aziz MS, Shaheen MS, El-Nekeety AA, Abdel-Wahhab MA. Antioxidant and antibacterial activity of silver nanoparticles biosynthesized using Chenopodium murale leaf extract. J Saudi Chem Soc. 2014;18(4):356-63. doi: 10.1016/j.jscs.2013.09.011.
28. Naik LS, Ramana Devi CV. Phyto-fabricated silver nanoparticles inducing microbial cell death via reactive oxygen species-mediated membrane damage. IET Nanobiotechnol. 2021 Oct;15(5):492-504. doi: 10.1049/nbt2.12036, PMID 34694754.
29. Liu L, Yu C, Ahmad S, Ri C, Tang J. Preferential role of distinct phytochemicals in biosynthesis and antibacterial activity of silver nanoparticles. J Environ Manage. 2023 Oct;344:118546. doi: 10.1016/j.jenvman.2023.118546, PMID 37418916.
30. Elsaffany AH, Abdelaziz AE, Zahra AA, Mekky AE. Green synthesis of silver nanoparticles using cocoon extract of Bombyx mori L.: therapeutic potential in antibacterial antioxidant anti-inflammatory and anti-tumor applications. BMC Biotechnol. 2025;25(1):38. doi: 10.1186/s12896-025-00971-9, PMID 40369507.
31. Wu J. The enhanced permeability and retention (EPR) effect: the significance of the concept and methods to enhance its application. J Pers Med. 2021 Aug;11(8):771. doi: 10.3390/jpm11080771, PMID 34442415.
32. Peng H, Zeng Y, Zhang R, Yang L, Wu F, Gai C. Cembranoid diterpenes from South China Sea soft coral Sarcophyton crassocaule. Mar Drugs. 2024;22(12):536. doi: 10.3390/md22120536, PMID 39728111.
33. Kornicka A, Balewski L, Lahutta M, Kokoszka J. Umbelliferone and its synthetic derivatives as suitable molecules for the development of agents with biological activities: a review of their pharmacological and therapeutic potential. Pharmaceuticals (Basel). 2023;16(12):1732. doi: 10.3390/ph16121732, PMID 38139858.
34. Alharbi NS, Felimban AI. Cytotoxicity of silver nanoparticles green-synthesized using Olea europaea fruit extract on MCF7 and T47D cancer cell lines. J King Saud Univ Sci. 2023 Oct;35(10):102972. doi: 10.1016/j.jksus.2023.102972.
35. Shakiba M, Rassouli FB. Joining up the scattered anticancer knowledge on auraptene and umbelliprenin: a meta-analysis. Sci Rep. 2024;14(1):11770. doi: 10.1038/s41598-024-62747-z, PMID 38783034.